Original paper

Verification of high-dose-rate brachytherapy treatment planning dose distribution using liquid-filled ionization chamber array

A.B. Mohamed Yoosuf, MSc[1], Prakash Jeevanandam, PhD[1], Glenn Whitten, MSc[1], Geraldine Workman, MSc[1], Conor K. McGarry, PhD[1,2]

[1]Department of Radiotherapy Medical Physics, Northern Ireland Cancer Centre, Belfast City Hospital, [2]Centre for Cancer Research and Cell Biology, Queen's University, Belfast, Northern Ireland, United Kingdom

Abstract

Purpose: This study aims to investigate the dosimetric performance of a liquid-filled ionization chamber array in high-dose-rate (HDR) brachytherapy dosimetry. A comparative study was carried out with air-filled ionization chamber array and EBT3 Gafchromic films to demonstrate its suitability in brachytherapy.

Material and methods: The PTW OCTAVIUS detector 1000 SRS (IA 2.5-5 mm) is a liquid-filled ionization chamber array of area 11 x 11 cm^2 and chamber spacing of 2.5-5 mm, whereas the PTW OCTAVIUS detector 729 (IA 10 mm) is an air vented ionization chamber array of area 27 x 27 cm^2 and chamber spacing of 10 mm. EBT3 films were exposed to doses up to a maximum of 6 Gy and evaluated using multi-channel analysis. The detectors were evaluated using test plans to mimic a HDR intracavitary gynecological treatment. The plan was calculated and delivered with the applicator plane placed 20 mm from the detector plane. The acquired measurements were compared to the treatment plan. In addition to point dose measurement, profile/isodose, gamma analysis, and uncertainty analysis were performed. Detector sensitivity was evaluated by introducing simulated errors to the test plans.

Results: The mean point dose differences between measured and calculated plans were 0.2% ± 1.6%, 1.8% ± 1.0%, and 1.5% ± 0.81% for film, IA 10 mm, and IA 2.5-5 mm, respectively. The average percentage of passed gamma (global/local) values using 3%/3 mm criteria was above 99.8% for all three detectors on the original plan. For IA 2.5-5 mm, local gamma criteria of 2%/1 mm with a passing rate of at least 95% was found to be sensitive when simulated positional errors of 1 mm was introduced.

Conclusion: The dosimetric properties of IA 2.5-5 mm showed the applicability of liquid-filled ionization chamber array as a potential QA device for HDR brachytherapy treatment planning systems.

Purpose

Modern brachytherapy is a sophisticated treatment modality embracing the use of standard high-dose-rate (HDR) after-loading equipment, combined with technological advances such as multi-modality imaging, applicator modelling, inverse planning optimization, and model-based dose calculation algorithms, which have paved the way for image-guided and adaptive brachytherapy [1,2,3,4,5,6]. Besides the ability to provide highly conformal doses to the target and minimizing dose to organs at risk (OAR), combined with a better understanding of radiobiological effects, brachytherapy is highly adaptable and can be used as a primary, adjunct, or salvage treatment [1]. Until recently, treatment planning systems (TPS) have been based on the hypothesis that tissue heterogeneity, applicator, and inter-source effects are negligible. Hence, dosimetry based on a water phantom was utilized for treatment planning calculations [7,8]. However, it is now clear that these factors do introduce uncertainties in the treatment planning process and new algorithms have been developed to account for them [1,9,10,11]. This will also require new verification techniques.

Brachytherapy dose delivery depends on the correct use of calibrated sources and dosimetric model for dose calculations. In order to prevent errors that might lead to a radiation incident, the need to accurately verify dose distributions calculated by the TPS has in-

creased extensively with the advent of image-guided brachytherapy and complex treatments that includes patient specific optimization to deliver a very high-dose of up to 15 Gy in a single fraction [12]. This raises the significance of having dosimetric systems that are able to measure the dose precisely in a specific point or plane from a given calibrated source to confirm that the intended dose is delivered to the patient. However, the current recommended quality control measures are limited to basic functions of the delivery system [13]. Hence, there is a need for more accurate verification of dose calculation as well as reliable quality assurance (QA) system and procedures. The measurement of dose distributions around HDR sources is challenging due to its multi-energy emanation and dose fall-off within a short distance. A millimeter displacement of the measuring point at the depth of interest due to positional uncertainties may yield an error of up to 13% in the measured value [13].

Due to its high spatial resolution and water equivalence, Gafchromic films (Ashland ISP Advanced Materials, NJ, USA) have been extensively used for dose verification of HDR brachytherapy dosimetry [14,15,16,17,18]. Furthermore, multichannel dosimetry provides an inherently improved calibration response, in addition to mitigate the specific potential source of uncertainty that includes thickness of the active layer, fingerprint abrasions, and dirt from the dose image [19,20,21]. However, Gafchromic films involve consumable cost and practical challenges like characterization of film and scanner to achieve accurate dosimetric results [8,22,23].

In recent years, various 2D and 3D ionization chamber arrays have become available, allowing for absolute and relative dose verification with real time outcomes, resulting in streamlined QA. Previous studies have investigated the use of the MatriXX 2D ionization array (IBA Dosimetry, Germany), and found it to be reliable for the measurement of absolute and relative dose distributions for the ^{192}Ir brachytherapy HDR source [23,24]. The PTW OCTAVIUS detector 729 (IA 10 mm) (PTW, Freiburg, Germany) and PTW OCTAVIUS detector 1000 SRS (IA 2.5-5 mm) (PTW, Freiburg, Germany) arrays have been used extensively for the verification of intensity modulated radiotherapy (IMRT), volumetric modulated arc therapy (VMAT), and stereotactic ablative body radiotherapy (SABR) treatment plans in external beam radiation therapy [25,26]. Recent studies have critically evaluated both arrays (IA 10 mm and IA 2.5-5 mm) and reported their sensitivity to detect multi-leaf collimator positional errors down to 1 mm in external beam radiotherapy [27,28,29,30]. No literature has been reported on the utilization of the IA 2.5-5 mm liquid-filled ionization chamber arrays in brachytherapy dosimetry. Most of the commercial array detectors are generally based on vented ion chambers. However, IA 2.5-5 mm is a liquid-filled ionization array that enables a reduced detector volume, due to the much higher density of the sensitive medium compared to air, which results in a narrower lateral dose response function in comparison to vented ion chambers [29].

In this work, the dosimetric performance of liquid-filled ionization chamber array (IA 2.5-5 mm) and its merits in comparison to vented ionization array (IA 10 mm) and Gafchromic EBT3 film has been studied.

Material and methods

Gafchromic film dosimetry

In this study, EBT3 Gafchromic film (Ashland Inc., Wayne, NJ) from a single batch (SN-09161402) was used. The scanning and handling protocol has been previously reported [21]. The calibration and the measurement films were marked to maintain the same orientation at scanning. All films were scanned 48 hours after irradiation using the Epson Expression 10000XL flatbed color scanner (Seiko Epson Corp., Nagano, Japan) in transmission mode, using 48 bits RGB (red, green, and blue) and 72 dpi (dots per inch) resolutions without any color corrections. Both irradiations and scanning were performed at room temperature.

EBT3 film was cut into 12 pieces of 4 cm x 10 cm and exposed to dose ranges between 0.5 and 6 Gy. A 6 MV photon beam using a Truebeam linear accelerator (Varian, Palo Alto, CA), which was calibrated using IPEM (Institute for Physics and Engineering and Medicine) code of practice traceable to primary standard (National Physics Laboratory – Teddington, UK), was utilized for EBT3 film calibration as it is a method consistent with previous publications and national brachytherapy audits [10,13,17,18,19,30,31,32]. Each calibration film was positioned at the center of the field of 10 cm x 10 cm at the depth of 5 cm in a WTe (water equivalent) solid water phantom (Barts and The London NHS Trust, London, UK), with 100 cm source to surface distance. The calibration and the measurement films were exposed within a narrow time window to avoid any inconsistencies in the film scanner compared to calibration scans [13]. FilmQA™ Pro (Ash-
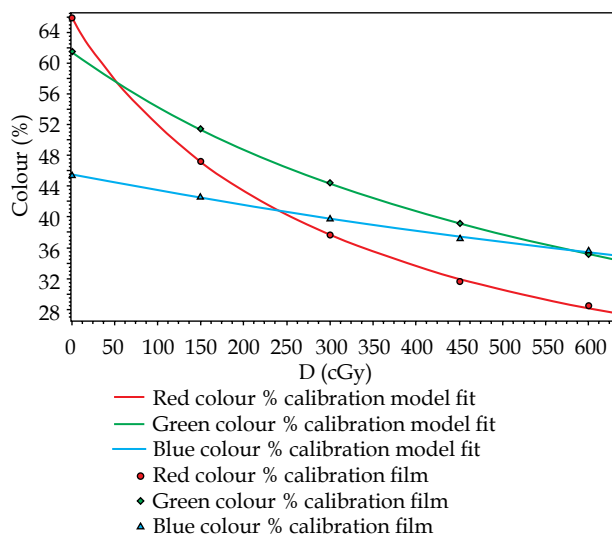

Fig. 1. Calibration curve for the Gafchromic EBT3 film used in this work

land, Inc., Wayne, NJ) software was used to analyze all scanned films [19]. The measurement film images were converted to dose maps using triple channel algorithm (FilmQA™ Pro software). Further, mean film pixel values in a 3 x 3 cm² region on the central axis of the beam were used for calibration. Figure 1 illustrates the multi-channel calibration curve derived using FilmQA Pro software. All analysis was performed using the red color channel for the experimental films due to its highest sensitivity for the dose levels of interest.

PTW OCTAVIUS

Detector 729 (IA 10 mm)

The IA 10 mm (PTW, Freiburg, Germany) 2D detector array consists of 729 vented ionization chambers surrounded by polymethylmethacrylate (PMMA), arranged in a square plane with total detector area of 27 x 27 cm². The size of each detector is 5.0 x 5.0 x 5.0 mm³, and they are equally spaced at 1 cm center-to-center with effective point of measurement located at 7.5 mm below the surface of the array. The dimension of the 2D array 729 are 30 x 42 x 2.2 cm³ (W x D x H) and weighs approximately 5.7 kg [27].

Detector 1000 SRS (IA 2.5-5 mm)

The IA 2.5-5 mm (PTW, Freiburg, Germany) 2D detector array consists of 977 liquid-filled ionization chambers that are arranged in a square plane, and the size of each detector is 2.3 x 2.3 x 0.5 mm³ (volume = 0.003 cm³), with a total detector area of 11 x 11 cm². The spacing of the detector is 2.5 mm center-to-center in the high-resolution region (5.5 x 5.5 cm²), whereas 5 mm center-to-center in the remaining area. The linear dimension of the detector is 30 x 42 x 2.2 cm³ (W x D x H). The device weighs approximately 5.4 kg, and the effective point of measurement is located at 9 mm below the surface of the array [28,29]. The active medium in the detector is filled with isooctane and is operated at 1000 V to minimize charge loses due to recombination effects [29].

The 2D arrays were set-up with the help of positioning lasers in such a way that the central axis intersects the central detector of the array. The TPS dose distribution of the plane of interest (2 cm from the source plane to the effective point of measurement) was exported (TPS resolution – 1 mm, coronal plane) to VeriSoft analysis software v. 5.1 (PTW, Freiburg, Germany) using Digital Imaging and Communications in Medicine (DICOM) format. Both IA 10 mm and IA 2.5-5 mm detectors were controlled by VeriSoft software for measurement acquisition and analysis. This software enables evaluation tools such as profile comparison (horizontal, vertical, and diagonal), planar isodose overlay, and gamma analysis using global/local normalization. The registration of the calculated and measured dose distribution was performed in Verisoft by aligning the center of the dose calculation box to the central ionization chamber of the arrays.

Cross calibration

Both IA 2.5-5 mm and IA 10 mm are calibrated by the manufacturer, which involves the calibration of individual chambers under reference condition using ⁶⁰Co radiation source. The 2D arrays (IA 2.5-5 mm and IA 10 mm) were calibrated using a cross calibration procedure [26,33]. In this method, a known dose of 1 Gy was delivered using a single dwell position (¹⁹²Ir source) to a prescription point at 2 cm depth, and the response of the central detector was used to calculate a cross-calibration factor or k factor and this factor was applied to the entire matrix.

Planning and delivery

The measurement geometry included a dedicated polymethylmethacrylate (PMMA) slab of dimensions 30 cm x 30 cm x 1 cm designed with three grooved channels (diameter – 2 mm) 1 cm apart for positioning the applicators (Lumencath 6 French – 2 mm diameter). The geometry setup, prescription points, profile direction, and the calculated isodose from the treatment planning system are illustrated in Figure 2. All three detectors were initially validated by calculating a treatment time on the TPS to give a prescribed dose (1 Gy) to a point 2 cm from a single dwell position and measuring the dose at this point for the exposure time. The maximum dose measured in the plane of interest was 1.005 Gy (TPS).

The setups, for all three detectors, was scanned using GE helical computed tomography (CT) (GE Medical systems, Milwaukee, WI) using the standard slice thickness of 2.5 mm (field of view – whole set up; 120 kVp; 50-550 mA). Test plans with three active catheters to mimic brachytherapy gynecological treatment were created using Elekta Oncentra® Brachy treatment planning system v. 4.1 (Elekta Oncology Systems, Crawley, West Sussex, UK) with a 1 mm calculation grid size. Dose in the range of 1-2 Gy was prescribed to six patient points (normalized) at 2 cm from the source plane. The plan had 17 dwell positions (catheter separation – 1 cm; catheter 1 with 4 dwell position placed 1 cm apart; catheter 2 with 4 dwell position placed 1 cm apart; catheter 3 with 9 dwell position placed 1 cm apart) over three channels (distribution of dwell position as shown in Figure 2) with 2.5 mm step size. The maximum dose values recorded in the plane of interest (TPS) was 1.96 Gy and 3.92 Gy for the prescription dose of 1 Gy and 2 Gy, respectively. All detectors (film and arrays) were placed at 2 cm (effective point of measurement) from the source plane for 2D dose measurement and a 5 cm solid water WTe (30 x 30 x 5 cm³) for backscatter was placed on both sides of the measurement assembly. TPS dose calculations were performed using Task Group No. 43 recommendations and the presence of applicator, inhomogeneities were not considered in the calculation. The TG-43 data are generally obtained from Monte Carlo (MC) radiation transport simulations in order to estimate the dosimetry around single HDR source. A Nucletron microSelectron HDR treat-
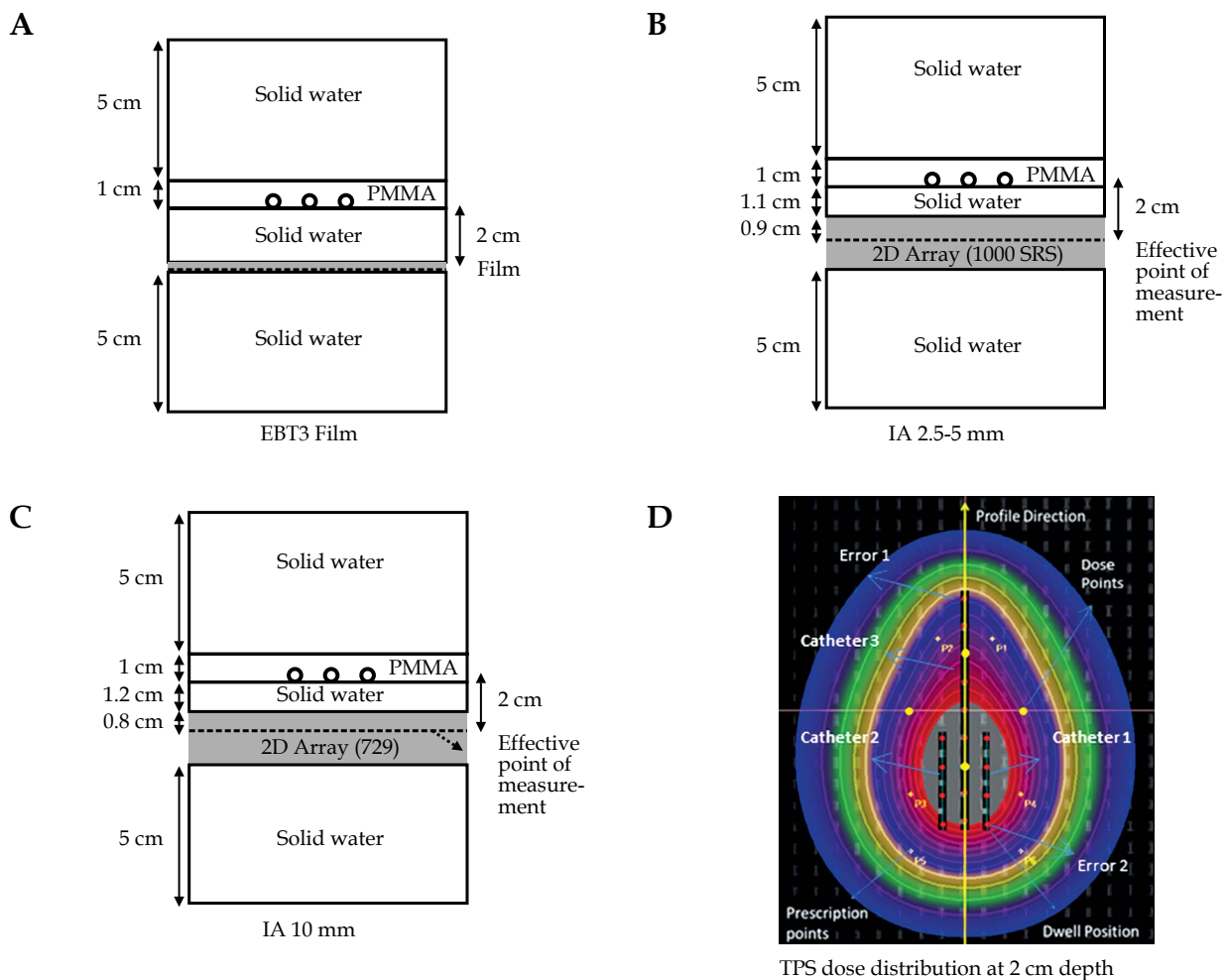
Fig. 2. Measurement geometry for film (**A**), IA 2.5-5 mm (**B**), IA 10 mm (**C**), and isodose distribution on the plane of interest in treatment planning systems (TPS) (**D**). TPS calculated isodose at 2 cm depth along with prescription points and profile direction

ment unit v. 3 (Elekta Oncology Systems, Crawley, West Sussex, UK) was used to deliver the plan.

Evaluation metrics

Quality indices assessed between the measured and calculated plan included: absolute point dose measurement, dose profiles, gamma maps, qualitative analysis of isodose distribution, and 2D gamma analysis using both global and local normalizations. For point dose measurements, four points (x = ± 2 cm; y = ± 2 cm) were considered at the detector plane (2 cm depth), and dose measured in these points were compared to the TPS calculated dose. The planar isodose distribution and profiles measured at 2 cm depth using the film and arrays (IA 2.5-5 mm and IA 10 mm) were evaluated against the TPS calculation. To assess the ability of the detectors in comparing dose distributions, 2D gamma analysis was performed by normalizing both calculated and measured dose distributions to the maximum absolute dose from the TPS calculated dose distribution. In order to quantify the agreement in dose maps, dose differences (ΔD) in

the range of 1-3% and distance to agreement (DTA) differences in the range of 1-3 mm, with a passing rate of at least 95%, were evaluated over a region of 110 mm x 110 mm using global/local gamma analysis. A 10% lower dose limit threshold was applied for all three detectors to exclude the dose levels that are clinically irrelevant [33].

Sensitivity analysis

The original plan (TPS) was modified to simulate errors, by introducing 1 mm, 2 mm and 3 mm shift of all dwell positions, and further tested using extreme errors by omitting a dwell position in low- and high-dose gradient regions as described in Table 1. The rationale behind introducing positional errors is to study the sensitivity of the detectors due to subtle changes in the treatment delivery and in the treatment plan. The passing rates (global and local) of each criterion after introducing the error in the plan were evaluated and compared to the original plan. All measurements were repeated five times for consistency.

Table 1. Description of virtual errors introduced in the original plan

Error	Description
Error 1	Dwell position omitted in catheter 3 (Figure 1)
Error 2	Dwell position omitted in catheter 1 (Figure 1)
Error 3	All dwell positions shifted 1 mm (profile direction – Figure 1)
Error 4	All dwell positions shifted 2 mm (profile direction – Figure 1)
Error 5	All dwell positions shifted 3 mm (profile direction – Figure 1)

Results

Point dose, isodose, and profile comparison

The average point dose measured for a prescription dose of 1 Gy at 2 cm from a single dwell position was 1.006 Gy (± 4.0), 0.999 Gy (± 0.01), and 0.990 Gy (± 0.04) using film, IA 2.5-5 mm, and IA 10 mm, respectively. The average difference in point dose between the measured and calculated plans for film, IA 2.5-5 mm, and IA 10 mm were 0.20% ± 1.6, 1.82% ± 0.98, and 1.52% ± 0.81, respectively, with measured generally lower than the calculated. Figure 3 shows the isodose comparison between measured and planned dose distribution with all three detectors for the given test
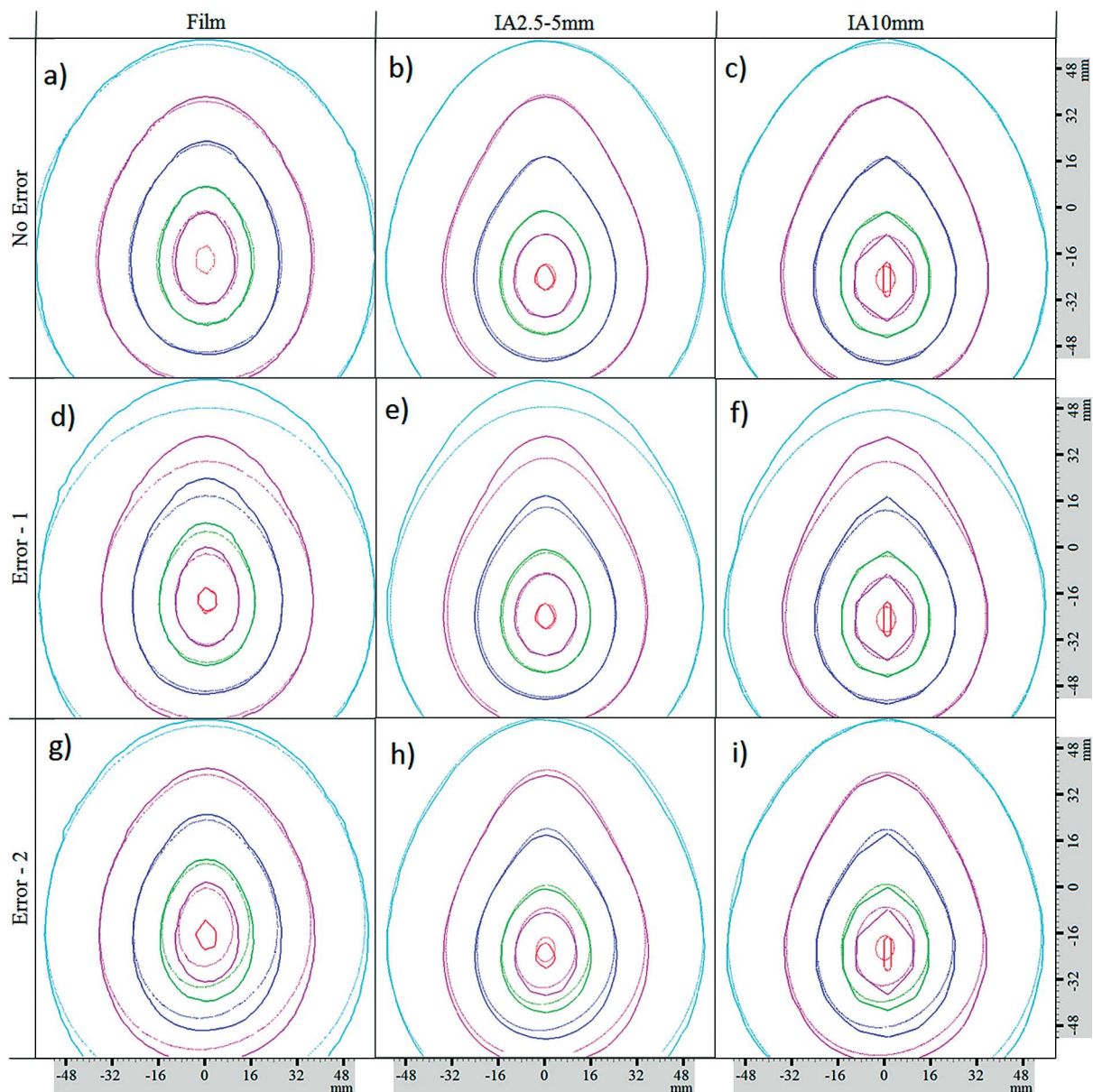

Fig. 3. Isodose comparison (1 Gy plan) between measured (solid line) and treatment planning systems (TPS) calculation (dashed line) for film, IA 2.5-5 mm, and IA 10 mm. Original plan (**A-C**); error 1 (**D-F**); error 2 (**G-I**). Isodose: 99% – red; 90% – purple; 80% – green; 60% – dark blue; 40% – pink and 20% light blue. Isodoses normalized to 1.96 Gy, maximum dose value in the plane of interest (TPS)

plans. As illustrated in Figure 3, the dose distributions measured using all three detectors was sensitive to simulated errors with IA 2.5-5 mm providing visibly better resolution than IA 10 mm. Similarly, good agreement was observed between measured and calculated dose profiles (direction of the profile as illustrated in Figure 2) for the original plan using all three detectors as shown in Figure 4. Furthermore, changes in profile shape due to simulated errors were observed. The k factor obtained for IA 2.5-5 mm and IA 10 mm detectors using ^{192}Ir HDR source are 0.999 and 1.081, whereas 0.945 and 1.041 were obtained using 6 MV photon beam, respectively.

Gamma analysis – original plans

Table 2 summarizes the gamma (median) comparison of measured and calculated dose distribution with all three detectors using both global and local gamma normalization for the test plans (original plan, error 1, and error 2). For original plan, average percentage of gamma pass rates using 2% ΔD and 2 mm DTA gamma criteria (global/local) was 99.8% ± 0.3/97.3% ± 1.3, 100% ± 0.1/99.4% ± 0.8, and 98.8% ± 0.4/91.2% ± 10.5 for film, IA 2.5-5 mm, and IA 10 mm, respectively. Similarly, gamma pass rates using 3% ΔD and 3 mm DTA gamma criteria (global/local) was 100.0% ± 0.0/100.0% ± 0.0, 100.0% ± 0.0/99.8% ± 0.3, and 99.8% ± 0.4/99.8% ± 0.4, respectively. Figure 5 illustrates the local gamma index maps using 3%/3 mm criterion for all plans using three detectors.

Sensitivity analysis

When simulated errors were introduced by omitting a dwell position in both low-dose gradient region
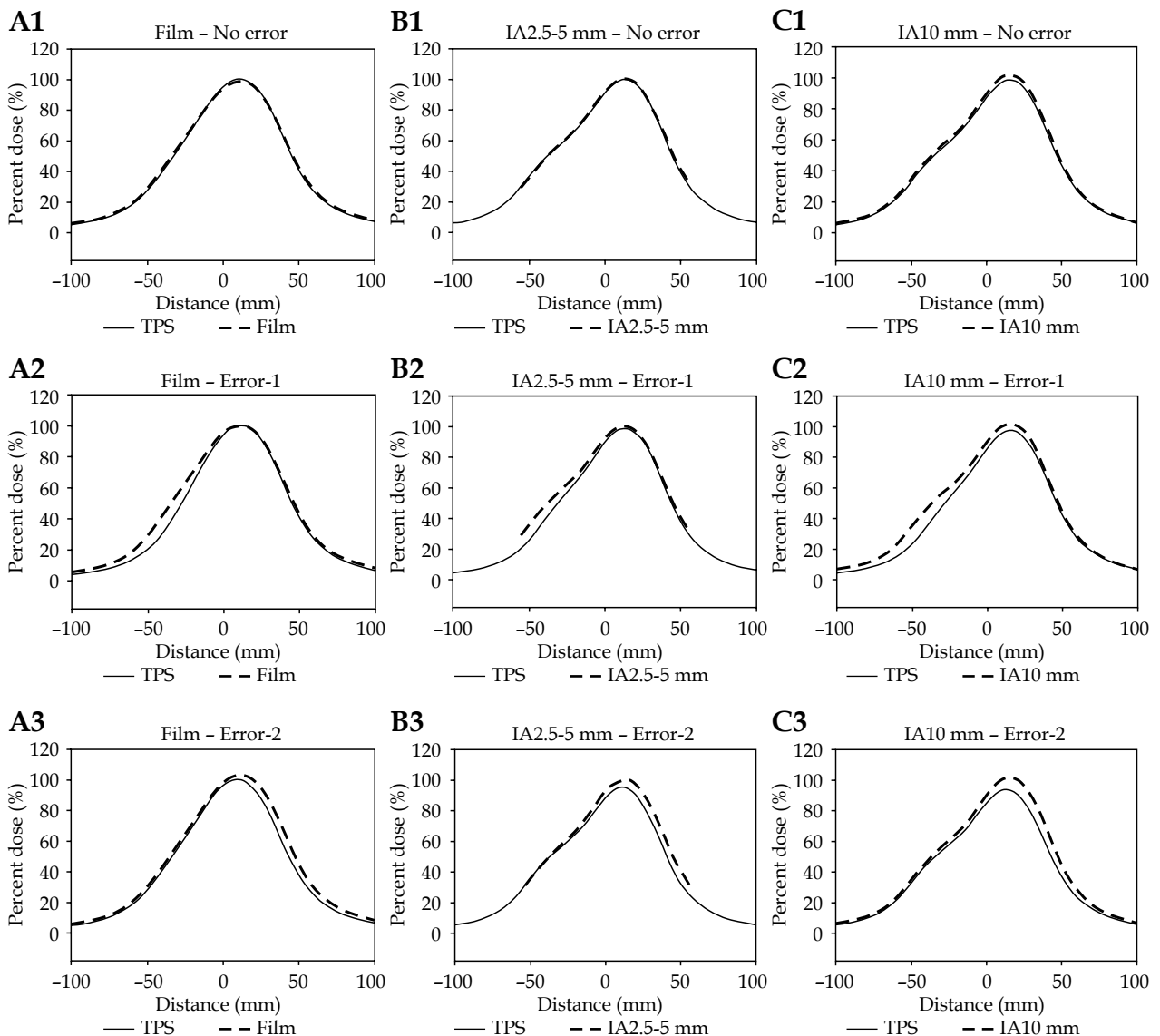

Fig. 4. Profile comparison between measured (dashed line) and treatment planning systems (TPS) calculation (solid line) for film, IA 2.5-5 mm, and IA 10 mm (all values normalized to maximum absolute dose calculated in TPS). Original plan (**A1-C1**); error 1 (**A2-C2**); error 2 (**A3-C3**)

Table 2. Gamma pass rates for range of criterions using all three detectors

	Gamma criterion	Film (passing rate) Median (± SD)		SRS 1000 (passing rates) Median (± SD)		729 (passing rates) Median (± SD)	
		Global	Local	Global	Local	Global	Local
Original Plan	3% 3 mm	100.0 ± 0.0	100.0 ± 0.0	100 ± 0.0	99.8 ± 0.3	99.8 ± 0.4	99.8 ± 0.4
	2% 2 mm	99.8 ± 0.3	97.3 ± 1.3	100 ± 0.1	99.4 ± 0.8	98.8 ± 0.4	91.2 ± 10.5
	2% 1 mm	95.3 ± 1.9	41.7 ± 17.4	99.3 ± 1.0	96.3 ± 4.9	96.5 ± 2.1	86.0 ± 0.9
	1% 1 mm	70.5 ± 5.3	23.9 ± 2.8	97.9 ± 1.7	93.5 ± 5.2	92.3 ± 1.1	80.5 ± 0.8
Error 1	3% 3 mm	83.2 ± 1.5	69.9 ± 2.2	89.5 ± 3.5	79.0 ± 3.4	84.0 ± 0.9	73.6 ± 0.8
	2% 2 mm	72.6 ± 2.1	61.3 ± 1.3	76.9 ± 3.2	64.8 ± 2.0	75.3 ± 1.8	65.0 ± 0.4
	2% 1 mm	64.1 ± 1.5	41.2 ± 3.1	63.9 ± 2.0	40.9 ± 6.9	67.7 ± 1.4	45.7 ± 1.3
	1% 1 mm	46.4 ± 1.8	25.6 ± 0.9	44.4 ± 6.6	37.1 ± 7.4	55.1 ± 1.2	42.8 ± 0.8
Error 2	3% 3 mm	91.9 ± 1.4	86.7 ± 1.9	91.4 ± 3.0	85.7 ± 4.8	89.7 ± 0.1	75.1 ± 0.8
	2% 2 mm	84.0 ± 2.0	67.5 ± 6.8	80.4 ± 4.9	70.6 ± 9.5	77.5 ± 0.6	57.1 ± 5.9
	2% 1 mm	69.4 ± 4.7	22.1 ± 2.0	63.6 ± 9.5	38.1 ± 15.6	67.9 ± 1.7	23.0 ± 7.6
	1% 1 mm	51.8 ± 26.3	10.5 ± 0.9	41.1 ± 13.7	30.6 ± 16.8	43.5 ± 6.1	18.3 ± 6.5

(error 1) and high-dose gradient region (error 2) of the original plan, all three systems showed sensitivity to errors with visible difference in the isodose/profile comparison (Figures 3 and 4) and reduced gamma passing rates (< 90%) using 3%/3 mm criterion (local/global) as shown in Table 2 and Figure 5.

Figure 6 illustrates the change in average (± SD) passing rates calculated using various ΔD/DTA (local/global) parameters due to positional error of 1 mm, 2 mm and 3 mm in the test plans (also see Table 3 – gamma pass rates for positional errors). Local normalization for gamma analysis was found to be more sensitive to positional errors. When a positional error of 1 mm was introduced in film, gamma (local) pass rates using 2% ΔD and 2 mm DTA were found to be sensitive with passing rates reduced from 97.3% ± 1.3 to 86.3% ± 4.6.

Similarly, for IA 2.5-5 mm, gamma (local) pass rates using 2% ΔD and 1 mm DTA criteria were sensitive to 1 mm error with passing rates reducing from 96.3% ± 2.5 to 82.2% ± 5.4. However, IA 10 mm achieved a gamma pass rate (using the same gamma criteria) of 86.0% ± 0.5 for the original plan and reduced to 70.9% ± 0.9, when a 1 mm error was introduced.

Evaluation of uncertainty

As the comparison of measured and calculated 2D dose distribution was considered the end result, standard uncertainty (calculated by combining type A and type B) for all three detectors were estimated and are shown in Table 4. The overall uncertainty was calculated as the square root of the sum of the squares of all the listed uncertainties. While the largest uncertainty was due to positional variability and phantom material, the overall uncertainty (coverage factor, $k = 1$) at the measurement depth (2 cm) was estimated as 4.75% for film dosimetry, with 2.31% and 2.19% for IA 10 mm and IA 2.5-5 mm, respectively.

Discussion

With the clinical implementation of more complex brachytherapy treatments, it is essential to routinely verify the dose calculated by treatment planning systems as well as the QA systems and procedures [34,35]. The clinical application of real time dose verification of high gradient beam profiles like those present in brachytherapy treatment plans, requires a detector with good repeatability, adequate sensitivity, dynamic range, and high spatial resolution [36]. Typical routine dosimetry involves an independent source position verification and dead-end measurement of catheters. In this study, we have shown that the array (IA 2.5-5 mm) investigated could be used to verify planar dose measurements against TPS calculations in brachytherapy dosimetry.

The EBT3 film was calibrated using 6 MV photon beams from a linear accelerator as this results in a more uniform radiation field than an ^{192}Ir source, and the setup is less sensitive to positioning and dose uniformity errors [31]. This methodology has previously been employed in a UK national audit [33]. We note that EBT3 Gafchromic film present significant energy response dependence on the low energy range with a difference of up to 20% and 5% was observed for 70 kVp and 300 kVp [37]. Gafchromic film dosimetry is an established technique for verifying two-dimensional dose distributions due to its high spatial resolution. However, film dosimetry requires great care and is time consuming if it is used as an absolute dosimeter.
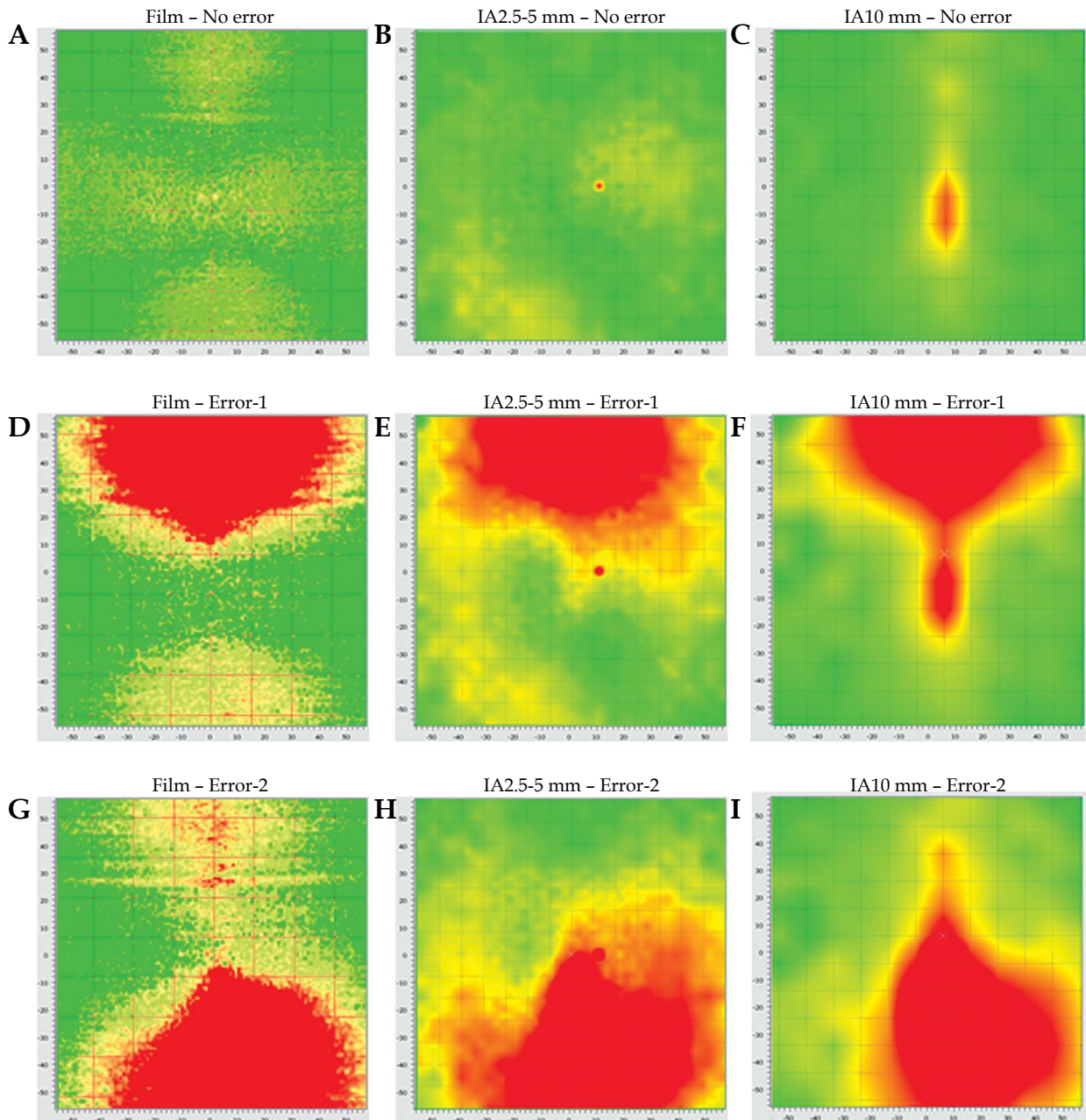
Fig. 5. Gamma maps (red – pixels failed; green – pixels passed) for film, IA 2.5-5 mm, and IA 10 mm. Original plan (**A-C**); error 1 (**D-F**); error 2 (**G-I**). Note: failing point in **B, E,** and **H** are due to dead pixel in OCTAVIUS 1000 SRS detector

Geometric uncertainties would influence the dose with respect to the dose gradient, thus relatively small geometric errors may have a significant consequence on the dose to target or organs at risk. The dose gradient in the intra-cavitary brachytherapy treatment technique is in the range of 5-12% per mm, at a distance of 1-3 cm from the source plane [38]. In addition, studies have reported that a deviation of 0.3 mm positioning error can lead to an uncertainty of the film dose value of up to 6.6% at 1.5 cm from the source [13,39]. The uncertainty at the current setup of 2 cm (source to detector distance) is expected to be less, however, not insignificant. Recent studies have also reported the influence

of non-water phantom material studied with respect to water for ^{192}Ir brachytherapy dosimetry [40,41,42]. Based on MC simulations, a difference of 0.59% has been observed between the dose measured in setup using water and phantom materials [14]. Nonetheless, the Gafchromic film continues to be the gold standard despite its drawbacks.

To our knowledge, this is the first study to document the application of liquid ionization arrays (IA 2.5-5 mm) in brachytherapy dosimetry. Previous studies have reported the use of vented ionization arrays, flat-panel imager, and diodes in brachytherapy, and found them to be reliable in verifying dwell posi-
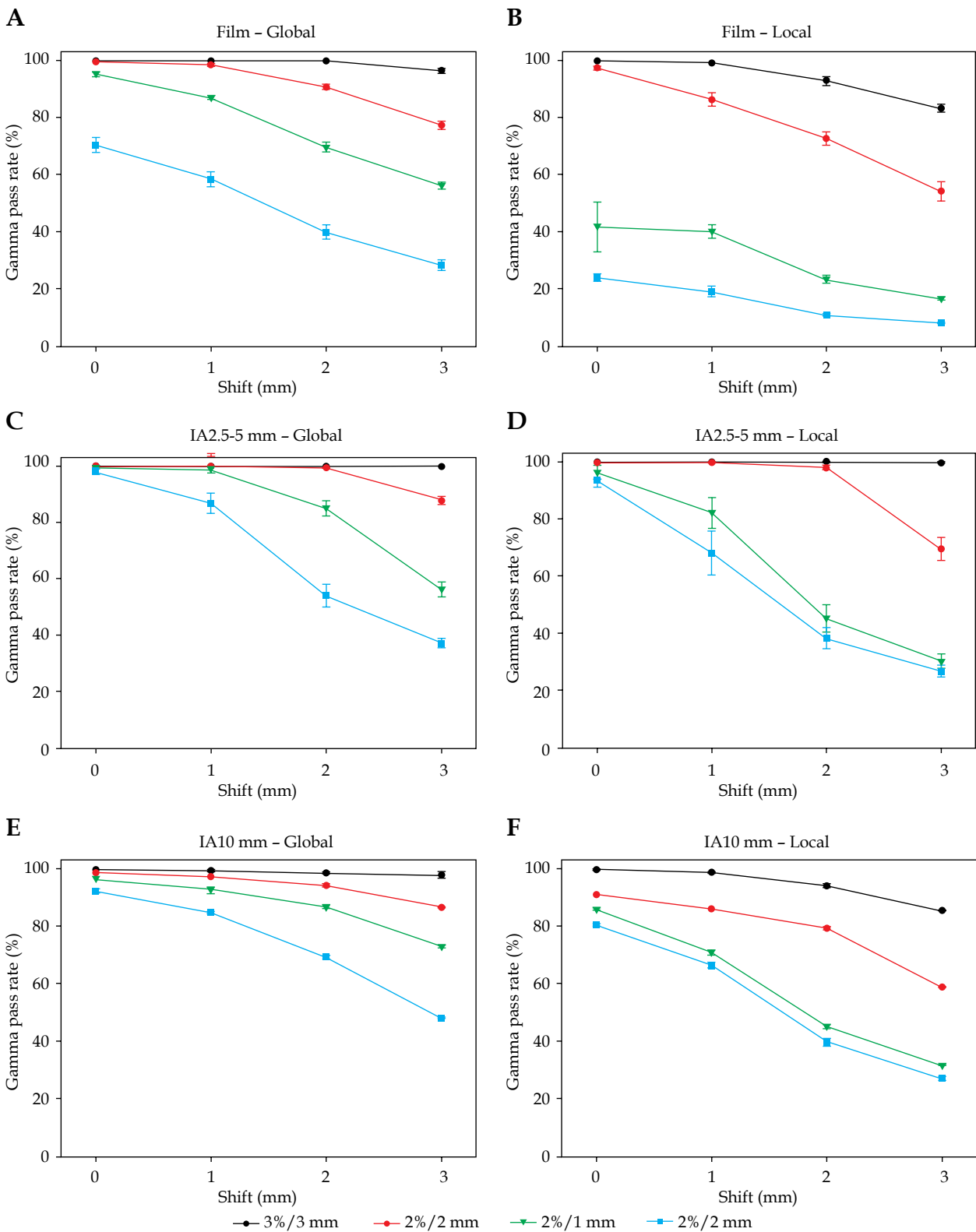
Fig. 6. Gamma pass rates for positional errors using all three detectors

tions and measuring absolute and relative dose distributions for the ^{192}Ir source [23,43,44,45,46]. Both IA 10 mm and IA 2.5-5 mm are well established, and have been routinely used for the verification of complex treatments like VMAT and SABR [25,26]. In this study, we have shown that a liquid-filled ionization-based array could be used effectively for the verification of brachytherapy plans created using commercial treat-

Table 3. Gamma pass rates for shift errors

	Gamma criterion	Film (passing rate) Median (± SD)		SRS 1000 (passing rates) Median (± SD)		729 (passing rates) Median (± SD)	
		Global	Local	Global	Local	Global	Local
Original plan	3% 3 mm	100.0 ± 0.0	100.0 ± 0.0	100 ± 0.0	99.8 ± 0.3	99.8 ± 0.4	99.8 ± 0.4
	2% 2 mm	99.8 ± 0.3	97.3 ± 1.3	100 ± 0.1	99.4 ± 0.8	98.8 ± 0.4	91.2 ± 10.5
	2% 1 mm	95.3 ± 1.9	41.7 ± 17.4	99.3 ± 1.0	96.3 ± 4.9	96.5 ± 2.1	86.0 ± 0.9
	1% 1 mm	70.5 ± 5.3	23.9 ± 2.8	97.9 ± 1.7	93.5 ± 5.2	92.3 ± 1.1	80.5 ± 0.8
1 mm Shift	3% 3 mm	100.0 ± 0.0	99.1 ± 1.1	100.0 ± 0.0	99.9 ± 0.1	99.5 ± 0.7	98.8 ± 0.4
	2% 2 mm	98.7 ± 1.0	86.3 ± 4.6	99.9 ± 0.0	99.7 ± 0.3	97.3 ± 0.4	86.2 ± 9.7
	2% 1 mm	87.1 ± 1.0	40.2 ± 5.1	98.6 ± 2.2	82.2 ± 10.7	93.1 ± 1.5	70.9 ± 1.8
	1% 1 mm	58.6 ± 4.9	19 ± 3.8	86.7 ± 7.3	68.1 ± 15.5	85.0 ± 0.2	66.5 ± 1.8
2 mm Shift	3% 3 mm	99.9 ± 0.1	92.9 ± 3.3	99.9 ± 0.1	99.9 ± 0.1	98.5 ± 0.7	94.1 ± 1.3
	2% 2 mm	90.8 ± 1.8	72.7 ± 4.6	99.4 ± 0.5	97.8 ± 1.4	94.3 ± 1.1	79.3 ± 0.5
	2% 1 mm	69.7 ± 3.7	23.4 ± 2.7	85.0 ± 5.4	45.2 ± 9.6	86.9 ± 1.1	45.2 ± 1.3
	1% 1 mm	40.1 ± 4.9	10.9 ± 0.6	54.0 ± 8.0	38.2 ± 7.4	69.4 ± 1.0	39.8 ± 2.8
3 mm Shift	3% 3 mm	96.4 ± 1.7	83.2 ± 3.0	99.8 ± 0.1	99.5 ± 0.3	97.8 ± 2.4	85.5 ± 0.2
	2% 2 mm	77.4 ± 2.9	54.2 ± 6.7	87.8 ± 3.0	69.5 ± 8.0	86.7 ± 0.1	59.0 ± 0.3
	2% 1 mm	56.3 ± 2.6	16.6 ± 1.1	56.2 ± 5.2	30.2 ± 5.2	73.1 ± 0.8	31.9 ± 0.1
	1% 1 mm	28.4 ± 3.5	8.1 ± 0.3	37.1 ± 3.2	26.7 ± 4.3	48.2 ± 0.5	27.2 ± 1.1

Table 4. Estimated standard uncertainties associated for each detector; EBT3 Gafchromic film, IA 2.5-5 mm and IA 10 mm

Source of uncertainty	Standard uncertainty ($k = 1$)				
	Film	IA 10 mm	IA 2.5-5 mm	References	Notes
Calibration of linear accelerator output for film calibration	0.5%	X	X	32	1
Film calibration fit function for creation of dose map in FilmQA Pro software	1.0%	X	X	13	2
Source strength calibration of HDR source	1.0%	1.0%	1.0%	50	3
TPS calculation	1.5%	1.5%	1.5%	7, 11, 18	4
Positional uncertainty	3.0%	1.0%	1.0%	13, 38, 39	5
Phantom material	3.0%	X	X	34	6
Scanning of film	0.2%	X	X	13, 21	7
Reproducibility	X	1.0%	0.5%	27, 28	8
Stability	X	0.2%	0.2%	28	9
Dose linearity	X	0.2%	0.5%	27, 28	10
Total uncertainty	4.75%	2.31%	2.19%		

1. Uncertainty in the calibration of linear accelerator output (6MV photon beam) measured using IPSM code of practice.
2. Estimated uncertainty from multichannel film calibration using FilmQA Pro software.
3. Uncertainty in ¹⁹²Ir source strength calibration using IPEM code of practice.
4. Uncertainty in the calculation of absorbed dose in TPS due to TG-43 formalism.
5. Uncertainty in dose measurement due to the position of detectors from the HDR source plane.
6. Uncertainty in dose calculation due to the phantom material used (solid water, PMMA) in the experimental setup.
7. Uncertainty in reproducibility of the response of the flatbed scanner.
8. Uncertainty in detector's (IA 2.5-5 mm and IA 10 mm) reproducibility of the output.
9. Uncertainty due to leakage current stability measurement of the ionization chamber detectors (IA 2.5-5 mm and IA 10 mm).
10.Uncertainty due to the detector's (IA 2.5-5 mm and IA 10 mm) linearity with dose rate.

ment planning systems to assure dosimetric accuracy in delivery.

The 729 array has a sampling frequency of 0.1 mm^{-1} along each row with 729 chambers arranged in a 27 × 27 cm^2 grid pattern, whereas 1000 SRS with 977 liquid-filled ionization chambers, has 0.4 mm^{-1} in the inner 5 × 5 cm^2 along the central axis, and the rest of the 11 × 11 cm^2 measurement area has a sampling frequency of 0.2 mm^{-1}, respectively. Hence the higher spatial resolution of the IA 2.5-5 mm makes it better suited for brachytherapy treatment plan verification, although a reduction in the spatial resolution of the TPS dose grid size may be required to obey Nyquist theorem [47,48].

The sensitive medium (liquid – isooctane) of the IA 2.5-5 mm has a density of 0.691 g/cm^3 when compared to the air density in the common ionization chambers (1.3 mg/cm^3). This enhances the photon and electron interactions probabilities and results in much higher sensitivity than the air-filled ionization chambers [29].

The adequacy of the gamma index in detecting errors has been commonly accepted and is implemented into most analysis software. However, it is equally important to understand the specific criteria to be used for particular detectors. We note that the gamma criterion of 2% ΔD and 2 mm DTA (local), and 2% ΔD and 1 mm DTA was sensitive to positional error of 1 mm in the original plan (minimum passing rate of at least 95%) using film and IA 2.5-5 mm, respectively. In particular, we found that the isodose distributions with IA 2.5-5 mm were visibly smoother due to its higher spatial resolution, when compared to the IA 10 mm. We note, from Figure 6, IA 2.5-5 mm showed greater error detection sensitivity to positional errors over IA 10 mm with a larger reduction in gamma pass rates (global/local) from the original plan, especially for 2% ΔD and 1 mm DTA, and 1% ΔD and 1 mm DTA criteria. There were differences in pixel resolutions between measured and the calculated (TPS) dose distributions.

Limitations

Generally, the accuracy of ionization detector arrays is subject to the uncertainties due to volume averaging, limited resolution, and self-attenuation, which leads to concern about their sensitivity to errors [36]. Measurement using ionization chambers (IA 2.5-5 mm and IA 10 mm) exhibit some amount of volume averaging, particularly in steep dose gradients, which have not been taken into account. Further, the response of the ionization chambers (IA 2.5-5 mm and IA 10 mm) with respect to directional dependence may also have affected this work.

Previous studies have observed energy dependence of the response of the arrays, with air vented arrays being less energy dependent due to the graphite chamber electrodes as opposed to liquid-filled arrays that have metal electrodes [29]. However, the energy dependency of the arrays and the influence of the phantom material in the dose response are mitigated when a cross calibration method was used to determine *k*-user factor. In addition, higher gamma pass rates may have been achieved by the arrays due to the cross calibration using the HDR source. The uniformity of response across the detectors in the presence of ^{192}Ir source needs further investigation. Using a calibration method with an energy source similar to ^{192}Ir e.g., a kilo voltage X-ray beam (300 kVp) for measuring *k*-user factor, would be more appropriate.

Looe *et al*. reported the shift of effective point of measurement for various chambers determined experimentally using high energy photon and electron beams [49]. The study confirmed that effective point of measurement is constant throughout all depths from the build-up region to beyond the reference depth. However, the impact of ^{192}Ir energy on the effective point of measurement is outside the scope of this work and requires further investigation.

Nevertheless, it has been shown that the liquid-filled ionization chamber-based array could be used for commissioning and as a routine quality assurance tool to verify brachytherapy plans created using a commercial treatment planning system. We also have shown that the IA 2.5-5 mm was sensitive to simulated errors introduced in the treatment plan and delivery. Further, isodose/profiles, gamma analysis, and point doses should be used when evaluating errors. There is potential to use liquid-filled ionization arrays in the commissioning of brachytherapy treatment planning systems that are based on TG 186 model-based dose calculation algorithms and in verification of source path within ring applicators [8].

HDR brachytherapy is witnessing a dramatic change in terms of treatment planning that includes functional imaging for target definition, the use of inverse optimization for delivering high doses in a single fraction, integration of brachytherapy treatment with external beam radiotherapy (EBRT), and adaptive brachytherapy [50]. High doses delivered in a single fraction combined with tight margins require enhanced QA and a stringent focus on safety and accuracy throughout the process. Quality control using arrays has been clearly demonstrated as a useful tool for brachytherapy. This could be an integral part of independent brachytherapy dose verification, similar to IMRT and VMAT in EBRT, before introducing new complex techniques to increase confidence in patient safety.

Conclusions

This study shows that the IA 2.5-5 mm is dosimetrically suitable for brachytherapy treatment plan verifications. The detector was more sensitive to positional errors than IA 10 mm due to its higher spatial resolution and was comparable to film dosimetry. The results suggest that liquid-filled ionization chamber array is a more convenient tool compared to film and could potentially be used for dose distribution verification of HDR treatment plans.

Acknowledgement

Disclosure

The authors report no conflict of interest.

References

1. Papagiannis P, Pantelis E, Karaiskos P. Current state of the art brachytherapy treatment planning dosimetry algorithms. *Br J Radiol* 2014; 87: 20140163.
2. Guedea F. Perspectives of brachytherapy: patterns of care, new technologies, and "new biology". *Cancer Radiothérapie* 2004; 18: 434-436.
3. Viswanathan AN, Dimopoulos J, Kirisits C et al. Computed tomography versus magnetic resonance imaging based contouring in cervical cancer brachytherapy: results of a prospective trial and preliminary guidelines for standardized contours. *Int J Radiat Oncol Biol Phys* 2007; 68: 491-498.
4. Van den Bos W, Beriwal S, Velema L et al. Image guided adaptive brachytherapy for cervical cancer: dose contribution to involved pelvic nodes in two cancer centers. *J Contemporary Brachytherapy* 2014; 6: 21-27.
5. Schindel J, Zhang W, Bhatia SK et al. Dosimetric impacts of applicator displacements and applicator reconstruction-uncertainties on 3D image-guided brachytherapy for cervical cancer. *J Contemporary Brachytherapy* 2013; 5: 250-257.
6. Wiercińska J, Wronczewska A, Kabacińska R, Makarewicz R. Transition from Paris dosimetry system to 3D image-guided planning in interstitial breast brachytherapy. *J Contemp Brachytherapy* 2015; 7: 479-484.
7. Rivard MJ, Coursey BM, DeWerd LA et al. Update of AAPM Task Group No. 43 Report: A revised AAPM protocol for brachytherapy dose calculations. *Med Phys* 2004; 31: 633-674.
8. Perez-Calatayud J, Ballester F, Das RK et al. Dose calculation for photon-emitting brachytherapy sources with average energy higher than 50 keV: Report of the AAPM and ESTRO. *Med Phys* 2012; 39: 2904-2929.
9. Beaulieu L, Tedgren ÅC, Carrier J et al. Report of the Task Group 186 on model-based dose calculation methods in brachytherapy beyond the TG-43 formalism: Current status and recommendations for clinical implementation. *Med Phys* 2012; 39: 6208-6236.
10. Rivard MJ, Beaulieu L, Mourtada F. Enhancements to commissioning techniques and quality assurance of brachytherapy treatment planning systems that use model-based dose calculation algorithms. *Med Phys* 2010; 37: 2645-2657.
11. Kirisits C, Rivard MJ, Baltas D et al. Review of clinical brachytherapy uncertainties: Analysis guidelines of GEC-ESTRO and the AAPM. *Radiother Oncol* 2014; 110: 199-212.
12. Zaorsky NG, Davis BJ, Nguyen PL et al. The evolution of brachytherapy for prostate cancer. *Nat Rev Urol* 2017; 14: 415-439.
13. Palmer AL, Nisbet A, Bradley D. Verification of high dose rate brachytherapy dose distributions with EBT3 Gafchromic film quality control techniques. *Phys Med Biol* 2013; 58: 497-511.
14. Aldelaijan S, Mohammed H, Tomic N et al. Radiochromic film dosimetry of HDR (192)Ir source radiation fields. *Med Phys* 2011; 38: 6074-6083.
15. Sharma SD, Bianchi C, Conte L et al. Radiochromic film measurement of anisotropy function for high-dose-rate Ir-192 brachytherapy source. *Phys Med Biol* 2004; 49: 4065-4072.
16. Evans M, Devic S, Podgorsak EB. High dose-rate brachytherapy source position quality assurance using radiochromic film. *Med Dosim* 2007; 32: 13-15.
17. Devic S, Tomic N, DeBlois F. Brachytherapy TPS QA using EBT model GafChromic film. *Med Phys* 2009; 36: 2528.
18. Palmer AL, Diez P, Gandon L et al. A multicentre 'end to end' dosimetry audit for cervix HDR brachytherapy treatment. *Radiother Oncol* 2015; 114: 264-271.
19. Micke A, Lewis DF, Yu X. Multichannel film dosimetry with nonuniformity correction. *Med Phys* 2011; 38: 2523-2534.
20. Palmer AL, Bradley D, Nisbet A. Evaluation and implementation of triple-channel radiochromic film dosimetry in brachytherapy. *J Appl Clin Med Phys* 2014; 15: 280-296.
21. Niroomand-Rad A, Blackwell CR, Coursey BM et al. Radiochromic film dosimetry: recommendations of AAPM Radiation Therapy Committee Task Group 55. *Med Phys* 1998; 25: 2093-2115.
22. Chandraraj V, Stathakis S, Manickam R et al. Comparison of four commercial devices for RapidArc and sliding window IMRT QA. *J Appl Clin Med Phys* 2011; 12: 338-349.
23. Yewondwossen M. Characterization and use of a 2D-array of ion chambers for brachytherapy dosimetric quality assurance. *Med Dosim* 2012; 37: 250-256.
24. Zeman J, Valenta J, Gabris F et al. Feasibility of MatriXX 2D detector array for HDR brachytherapy planning system assessment. *Metrologia* 2012; 49: S237-240.
25. McGarry CK, O'Connell BF, Grattan MWD et al. Octavius 4D characterization for flattened and flattening filter free rotational deliveries. *Med Phys* 2013; 40: 091707.
26. Hussein M, Adams EJ, Jordan TJ et al. A critical evaluation of the PTW 2D-ARRAY seven29 and OCTAVIUS II phantom for IMRT and VMAT verification. *J Appl Clin Med Phys* 2013; 14: 274-292.
27. Spezi E, Angelini A L, Romani F, Ferri A. Characterization of a 2D ion chamber array for the verification of radiotherapy treatments. *Phys Med Biol* 2005; 50: 3361-3373.
28. Markovic M, Stathakis S, Mavroidis P et al. Characterization of a two-dimensional liquid-filled ion chamber detector array used for verification of the treatments in radiotherapy. *Med Phys* 2014; 41: 051704.
29. Poppe B, Stelljes TS, Looe HK et al. Performance parameters of a liquid filled ionization chamber array. *Med Phys* 2013; 40: 082106.
30. Sukumar P, McCallum C, Hounsell AR et al. Characterisation of a two-dimensional liquid-filled ion chamber detector array using flattened and unflattened beams for small fields, small MUs and high dose-rates. *Biomed Phys Eng Express* 2016; 2: 025007.
31. Palmer AL, Lee C, Ratcliffe AJ et al. Design and implementation of a film dosimetry audit tool for comparison of planned and delivered dose distributions in high dose rate (HDR) brachytherapy. *Phys Med Biol* 2013; 58: 6623-6640.
32. Lillicrap S C, Owen B, Williams J R et al. Code of practice for high-energy photon therapy dosimetry based on the NPL absorbed dose calibration service. *Phys Med Biol* 1990; 35: 1355-1360.
33. Hussein M, Tsang Y, Thomas RAS et al. A methodology for dosimetry audit of rotational radiotherapy using a commercial detector array. *Radiother Oncol* 2013; 108: 78-85.
34. Fraass B, Doppke K, Hunt M et al. American Association of Physicists in Medicine Radiation Therapy Committee Task Group 53: quality assurance for clinical radiotherapy treatment planning. *Med Phys* 1998; 25: 1773-1829.
35. Granero D, Vijande J, Ballester F et al. Dosimetry revisited for the HDR 192Ir brachytherapy source model Mhdr-v2. *Med Phys* 2011; 38: 487-494.

36. DeWerd LA, Ibbott GS, Meigooni AS. et al. A dosimetric uncertainty analysis for photon-emitting brachytherapy sources: Report of AAPM Task Group No. 138 and GEC-ESTRO. *Med Phys* 2011; 38: 782-801.

37. Villareal-Barajas JE, Khan RF. Energy response of EBT3 radiochromic films: implications for dosimetry in kilovoltage range. *J Appl Clin Med Phys* 2014; 15: 331-338.

38. Hellebust TP, Kirisits C, Berger D et al. Recommendations from Gynaecological (GYN) GEC-ESTRO Working Group: Considerations and pitfalls in commissioning and applicator reconstruction in 3D image-based treatment planning of cervix cancer brachytherapy. *Radiother Oncol* 2010; 96: 153-160.

39. Palmer AL, Bradley DA, Nisbet A. Evaluation and mitigation of potential errors in radiochromic film dosimetry due to film curvature at scanning. *J Appl Clin Med Phys* 2015; 16: 425-431.

40. Hermida-Lopez M, Ludemann L, Fluhs A et al. Technical Note:Influence of the phantom material on the absorbed-dose energy dependence of the EBT3 radiochromic film for photons in the energy range 3 keV-18MeV. *Med Phys* 2014; 41: 112103.

41. Schoenfeld A, Harder D, Poppe B et al. Water equivalent phantom materials for ^{192}Ir brachytherapy. *Phys Med Biol* 2015; 60: 9403-9420.

42. McEwen MR, DuSautoy. Characterization of the water- equivalent material WTe for use in electron beam dosimetry. *Phys Med Biol* 2003; 48: 1885-1893.

43. Asgharizadeh S, Bekerat H, Syme A et al. Radiochromic filmebased quality assurance for CT-based high-dose-rate brachytherapy. *Brachytherapy* 2015; 14: 578-585.

44. Espinoza A, Beeksma B, Petasecca M et al. The feasibility study and characterization of a two dimensional diode array in "magic phantom" for high dose rate brachytherapy quality assurance. *Med Phys* 2013; 40: 111702.

45. Miyahara Y, Kitagaki H, Nishimura T et al. Usefulness of direct-conversion flat-panel detector system as a quality assurance tool for high-dose-rate ^{192}Ir source. *J Appl Clin Med Phys* 2015; 16: 121-129.

46. Manikandan A, Biplab S, David PA et al. Relative dosimetrical verification in high dose rate brachytherapy using two dimensional detector array IMatriXX. *J Med Phys* 2011; 36: 171-175.

47. Stelljes TS, Harmeyer A, Reuter J et al. Dosimetric characteristics of the novel 2D ionization chamber array OCTAVIUS Detector 1500. *Med Phys* 2015; 42: 1528-1537.

48. Poppe B, Djouguela A, Blechschmidt A et al. Spatial resolution of 2D ionization chamber arrays for IMRT dose verification: single-detector size and sampling step width. *Phys Med Biol* 2007; 52: 2921-2935.

49. Looe HK, Harder D, Poppe B. Experimental determination of the effective point of measurement for various detectors used in photon and electron beam dosimetry. *Phys Med Biol* 2011; 56: 4267-4290.

50. Thomadsen BR, Erickson BA, Eifel PJ et al. A Review of Safety, Quality Management, and Practice Guidelines for High-Dose-Rate Brachytherapy. *Pract Radiat Oncol* 2014; 4: 65-70.